Accurate Indoor Positioning Using Temporal-Spatial Constraints Based on Wi-Fi Fine Time Measurements

Wenhua Shao, Haiyong Luo, Fang Zhao, Hui Tian, Shuo Yan, Antonino Crivello

Abstract—The IEEE 802.11mc-2016 protocol enables certified devices to obtain precise ranging information using time-of-flight based techniques. The ranging error increases in indoor environments due to the multipath effect. Traditional methods utilize only the ranging measurements of the current location, thus limiting the abilities to reduce the influence of multi-path problems. This paper introduces a robust positioning method that leverages the constraints of multiple positioning nodes at different positions. We transfer a sequence of temporal ranging measurements into multiple virtual positioning clients in the spatial domain by considering their spatial constraints. Defining an objective function and the spatial constraints of the virtual positioning clients as Karush–Kuhn–Tucker conditions, we solve the positioning estimation with non-convex optimization. We propose an iterative weight estimation method for the time of flight ranging and the virtual positioning client to optimize the positioning model. An extensive experimental campaign demonstrates that our proposal is able to remarkably improve the positioning accuracy in complex indoor environments.

Index Terms—indoor positioning, Wi-Fi positioning, fine time measurements, Internet of Things, IEEE 802.11mc-2016

I. INTRODUCTION

INDOOR location-based services (LBS) have received increasing attention due to the high demand for location-aware applications [1-4]. Wireless local area network (WLAN) based localization methods are attractive owing to their advantages of ubiquitous and open access. Generally, the positions of already installed Wi-Fi access points (APs) are unknown and the low accuracy of distance estimation in the log-distance path loss (LDPL) model, most of the WLAN positioning methods rely on fingerprinting methods [5-7]. The fingerprinting methods improve positioning accuracies, but the method also requires sample signal fingerprints of each point in the map and to update the fingerprint database periodically, therefore the cost of the fingerprint method is too expensive to be applied in a large area.

In order to improve the positioning ability of WLAN, researchers propose the IEEE 802.11mc fine time measurement (FTM) protocol in 2016 [8]. The protocol enables certified devices to precise ranging with the time-of-flight (ToF) technique. Intel reports that, based on their chip, the one sigma ranging accuracy and the positioning accuracy reach 1.4m and 2m respectively in line of sight (LoS) environments [9]. Considering that the ranging accuracy decides the positioning accuracy in trilateration localization, Ibrahim et al. [10] verified the ranging performance in indoor and outdoor environments. Their experiments reveal that the indoor ranging accuracy is much lower than in outdoor environments due to the multipath problem which prevents the Wi-Fi chip to precisely decide the arrival time of the ranging request. Therefore, research on FTM indoor positioning faces several challenges for improving indoor positioning accuracy.

In order to attenuate the multi-path interferences, classical ranging systems averaging multiple measurements on the same location. This operation helps filter out sensor noises, but cannot eliminate the multipath effect which leads to distance overestimation. Authors in [10] build a window of 10 bursts which each being 30 packets long, then estimate the most probable distance by building a histogram for each window. The method improves positioning accuracy, but it is difficult to be used in moving objects because the client only gets one observation at each location. Considering that the ranging error is mainly caused by multipath problems, therefore is location

Wenhua Shao is with the School of Software Engineering, and the School of Information and Communication Engineering, Beijing University of Posts and Telecommunications, Beijing, 100876, China. (e-mail: shaowenhua@ict.ac.cn).

Haiyong Luo is with the Institute of Computing Technology, and Beijing Key Laboratory of Mobile Computing and Pervasive Device, Chinese Academy of Sciences, Beijing, 100876, China (e-mail: yhluo@ict.ac.cn).

Fang Zhao is with the School of Software Engineering, Beijing University of Posts and Telecommunications, Beijing, 100876, China. (e-mail: zfsse@bupt.edu.cn).

Hui Tian is with the School of Information and Communication Engineering, Beijing University of Posts and Telecommunications, Beijing, 100876, China. (e-mail: tianhui@bupt.edu.cn).

Shuo Yan is with the School of Software Engineering, Beijing University of Posts and Telecommunications, Beijing, 100876, China. (e-mail: lightning@bupt.edu.cn).

Antonino Crivello is with the Institute of Information Science and Technologies, CNR, Italy. (e-mail: antonino.crivello@isti.cnr.it).

related, we affirm that leveraging the observations at different places reduces the side effect caused by the multipath problem. We transfer a sequence of ranging measurements in the temporal domain into multiple virtual positioning clients (VPCs) in the spatial domain. Then, these VPCs are connected with spatial constraints. Because the multipath effect varies at different locations, we convert the real-time position estimation problem into multiple VPCs combined position optimization, by constructing a multipath reduction model evaluating VPCs at different locations.

Another challenge is due to the diversity and the complexity of the available positioning information when considering multiple VPCs. For example, the estimated accuracy of VPC moving distance varies for different kinds of positioning clients; an optimal position estimation needs to consider the ranging accuracy between different VPCs and Wi-Fi access point (AP) pairs; the available number of ranging measurement and positioning ability of each VPC also varies. Therefore, we model the VPCs positioning as a non-convex optimization problem with multiple constraints, then we solve it with the Karush–Kuhn–Tucker (KKT) conditions [11]. The proposed method successfully combines multiple positioning constraints, therefore improves the positioning accuracy and its robustness.

The third challenge is how to estimate the quality of ranging measurements and that of each VPC positioning accuracy using only a few observations at each point. Considering the complexity of the ranging error distribution for each point, it is too difficult to precisely compute their distributions respectively. Therefore, considering the environment similarity of a building, we propose that using one identical distribution to approximate all the ranging errors of the same building. Then based on ranging measurement residuals, we can adopt mean/median estimation for these measurements with only a few measurements. Based on robust statistics theory [12], we transfer the mean/median estimation into ranging weights. We also propose that the sum of all the ranging weights of one VPC contains both available ranging APs and ranging qualities, therefore it can be used as an indicator of VPC positioning quality. Finally, weight estimations are iteratively updated when position estimations are updated. The proposed dynamic weight updating method improves the robustness of dealing with poor FTM ranging measurements and poor VPCs whose all ranging measurements are influenced.

Specifically, we provide the following contributions:

- To attenuate the side effect of the multipath problem in complex indoor environments, we propose to transfer a ranging sequence into VPCs, and to leverage the spatial constraints to combine observations at multiple locations, consequently improves the robustness.
- In order to tackle the diversity and complex positioning information from multiple VPCs, we propose a positioning KKT condition model that integrates the information from VPC spatial constraint, ranging quality and VPC positioning quality.
- To estimate the ranging measurement and VPC positioning quality, we establish the ranging measurement model and iteratively updates the quality weight, which improves the

system robustness of dealing poor ranging measurements and VPCs.

The rest of the paper is organized as follows. Related work is reviewed in Section II. Section III introduces the challenges and the system overview and the overall positioning algorithm. The details of the proposed temporal-spatial optimization models are given in Section IV. Implementation details and experimental results are presented and discussed in Sections V. Finally, Section VI concludes this paper.

II. RELATED WORK

Many indoor positioning techniques have been presented over the past years, including magnetic field [13-15], acoustic [16], PDR [17, 18], camera [19], Bluetooth [20] and Wi-Fi [21-23]. Amongst all these techniques, the one that uses Wi-Fi infrastructure has attracted special attention due to the urgent need of internet access service in indoor environments. However, traditional Wi-Fi access points cannot provide precise ranging information, thus causing the Wi-Fi based positioning needs high site-survey cost but the positioning accuracy is poor. The recently proposed IEEE 802.11mc protocol enables Wi-Fi access point's ranging ability, consequently provides a new way to improve indoor positioning performance. Our work builds upon the FTM enabled Wi-Fi access points, and deals with the poor positioning performance problem in indoor environments.

From a position computation perspective of radio-based signaling systems, the Wi-Fi positioning approaches can be divided into three categories: (1) clustering; (2) weight estimation; (3) sparsity. The clustering method aims to select a subset of APs then estimate a rough positioning result with minimum computation costs. He [24] tries to mitigate the noise generated in fingerprint collection and target measurement, he proposes a spectral clustering-based method by mapping the target RSSI of each AP to a convex hull. Then he formulates a linear programming problem to localize targets. FreeLoc [5] method finds that crowdsourced Wi-Fi fingerprint suffers from short RSS measuring time and device heterogeneity problem. The method is based on the overall relationship among RSS by APs, therefore, improve the localization robustness in crowdsourced environments. Due to the instability of Wi-Fi signals, the performance of this kind of method decreases after a few months.

The weight estimation methods improve positioning accuracy by adjusting the distance between online measurements and RSS radio map fingerprints. Fang's algorithm [25] intelligently transforms RSS into principal components such that the information of all APs is more efficiently utilized. The technique replaces the elements with a subset of principal components to simultaneously improve the accuracy and reduce the online computation. Mirowski [26] considers the distribution for computing similarities among fingerprints using Kullback Leibler divergence, and that performs localization through kernel regression. The method provides a natural way of smoothing over time and trajectories. The weight estimation methods utilize the whole set of fingerprints, thus are more computationally complex. The

weight estimation methods are also based on Wi-Fi fingerprints, therefore also suffer from the performance instability problem.

The sparsity method tries to decrease the computational complexity while not traded off localization accuracy. Chen [27] finds that the sparse nature of localization makes compressive sensing desirable for accurate indoor environments using RSS. He recovers sparse signals from a small number of noisy measurements by solving an ℓ_1-minimization problem, which reduces the number of measurements significantly. Khalajmehrabadi [28] improves the performance by minimizes the ℓ_1-norm of the location vector and the ℓ_2-norm of the residuals. The sparsity methods are usually designed to suit specific environments; therefore, their availabilities are limited for pervasive environments.

In recent years, MIMO based positioning techniques have been presented showing accuracies under 1 meter in indoor environments. These techniques can be classified into two categories: Angle of Arrival (AoA) and Time of Arrival (ToA). AoA measurement determines the direction of propagation of a radio-frequency wave incident on an antenna array or determined from maximum signal strength during antenna rotation. ArrayTrack [29], pioneering in MIMO based Wi-Fi positioning, authors use a software-defined radio platform and up to 16 antennas for each AP. Later, Ubicarse [30] shows the application of synthetic aperture radar to improve accuracy. However, the method requires users to twist devices while they walk. More recently, SpotFi [31] and Phaser [32] successfully apply phased arrays on commodity APs. Several advances use the physical layer information to accurately deduce the ToA (i.e., the travel time of a radio signal from a signal transmitter to a remote single receiver), breaking the meter accuracy barrier. Splicer [33] combines channel state information (CSI) from multiple channels for accurate power delay profile. On the other hand, ToneTrack [34] further increases the accuracy by integrating the combination process with a super-resolution ToA estimation. Chronus [35] modifies the Wi-Fi card driver to support fast channel hopping. SiFi [36] presents a single AP-based positioning system able to reach accuracy under 1 meter with a single channel only.

Despite the high accuracies reached in the abovementioned works, unfortunately, the MIMO-based techniques require antenna arrays or multiple antennas to extract the CSI information, which limits the size of terminals and the manner to deploy the antennas. Another problem with CSI based localization is that the CSI packets require high bandwidth. Therefore, researchers are attempting to implement ranging-based positioning with round trip time (RTT) techniques, eliminating the requirement of antennas. Gunther [37] proposes a RTT method to estimate the distance between WLAN nodes without using additional hardware and achieves 8m ranging accuracy. Then, Ciurana [38] utilizes the available WLAN card clock at 44MHz achieving 1m of accuracy. Giustiniano [39] implements carrier sense-based ranging methods further improving the systems' accuracy also reaching an accuracy under 1 meter. Recently, Intel proposed the Wi-Fi ToF protocol [9] and related chips, providing an off-the-shelf way to implement high-accuracy indoor positioning. They propose

several articles based on the FTM ranging technology. In [40] authors integrate Wi-Fi FTM and inertial sensors with extended Kalman filter to harness each other's advantages. In [41] authors update the protocol with a collaborative time of arrival that enables an unlimited number of users to position themselves through Wi-Fi information. In [42] has been presented a supervised deep neural network able to outperforms the accuracies reached from classic maximum-likelihood estimation methods. In [43] authors conduct an extensive experimental campaign based on a customized Wi-Fi echo technique in order to understand the noise source which affects ToF measurements. Then, Rea [44] combines statistical learning and robust statistics in a single filter, that is better suited for the inherent large noise as found in Wi-Fi radios. Verification [10] introduces an open platform for experiments with FTM ranging. The authors analyze the key factors and parameters that affect the ranging performance and present that meter-level ranging accuracy can only be consistently achieved in low-multipath environments. Yu [45] proposes an unscented Kalman filter based dead reckoning algorithm to combine the results of Wi-Fi FTM and multiple sensors. Niesen [46] applies the Wi-Fi FTM ranging on the problem of range estimation between pairs of moving vehicles. He develops a range estimation algorithm using local polynomial smoothing of the vehicle motion.

As a summary, though FTM positioning accuracies under 1 meter can be achieved using, for example, trilateration in an outdoor environment [10]. Instead, in indoor complex scenarios, the positioning performance drops remarkably mainly due to the multi-path effect on the ranging measurements. The existing FTM based positioning techniques focus on improving performance considering a single Wi-Fi measurement and, eventually, integrating data from inertial sensors. Nevertheless, the positioning accuracy and applicable scenarios are limited. Differently from these studies, in this paper, we consider multiple previous FTM measurements also evaluating their relative spatial relations. Our approach is able to estimate ranging qualities, adjust measurement weights, and estimate the target positions using multiple FTM measurements. Furthermore, by identifying and decreasing the weight of poor ranging measurements, the proposed system remarkably improves positioning accuracy in complex indoor environments.

III. SYSTEM OVERVIEW

State-of-the-art positioning methods based on FTM RTT [9] leverage the latest ranging measurements to estimate the current position. The potential useful history of restrictions is generally discarded. In order to utilize historical information of the positioning client, we propose a based joint positioning method to jointly optimize the client's position. The section first introduces challenges for FTM ranging in indoor environments, then proposes the VPC concept to implement joint positioning. Finally, we introduce the system architecture.

A. Fine Time Measurement Ranging Challenges

The FTM protocol of the IEEE 802.11mc-2016 standard

enables certified products to measure each other's distances with the RTT method. The ranging method reaches sub-meter accuracy in ideal Line-of-Sight (LoS) environments [10], but the performance drops in complicated indoor environments. As Fig. 1 reveals, there are several factors that may affect the RTT ranging performance, but the most serious factors are the multipath effect and electromagnetic interference.
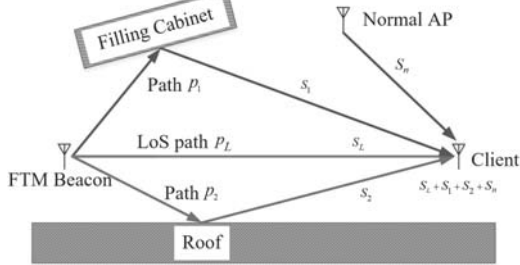

Fig. 1. Indoor challenges for FTM ranging.

The multipath effect is the problem that Wi-Fi signals propagate to the client by several paths, therefore arrive at the receiver at different times. As Fig. 1 reveals, when an FTM beacon sends a ranging frame to a client, the client not only receives signals from LoS path S_L but also reflected signals from other paths, for instance, roofs S_2 and filling cabinets S_1. Therefore, the actual received signal at the receiver is the sum of signals from different paths, that is $S_L + S_1 + S_2$. Because the length of propagation paths S_l, S_{p1} and S_{p2} are different, the ranging signal is divided into several pieces that arriving at the client at different times. Therefore, the multi-path effect introducing serious interferences to the client receiver, leading to a decrease of ranging accuracy.

On the other hand, a lot of Wi-Fi APs are deployed within indoor environments to fulfill communication requirements. However, these normal APs work in the same frequency of FTM ranging signals. These signals from normal APs S_n interferes with the wave shape of FTM ranging signals, thus decreasing the ranging accuracy. Consider all these interferences, it is difficult for the system to exactly determine the arrival time of FTM frames, therefore the ranging and positioning accuracy decrease in indoor environments.

B. Virtual Positioning Client Creation

The interference strength generally varies at different locations of the indoor environment. If several clients are in the same area and the distances between them are given, then positioning estimations can be improved by optimizing the ranging measurements of all the clients simultaneously. Fig. 2 show an example in which six location-known FTM beacons, namely $B_1 \sim B_6$,and two location-unknown clients, namely $C_1 \sim C_2$, have been placed in the indoor area. Client C_1 receives four ranging measurements from B_1, B_2, B_5, B_6. Due to the wall's attenuation, client C_2 receives only two measurements from B_3, B_4. A positioning algorithm, based on ranging measurements, will estimate the position of C_2 within a location area with an uncertainty, namely A_1. If the algorithm takes into account also the distance d between the two clients and the ranging measurements of C_1, then the area of uncertainty for

estimating the positioning of C_2 can be decreased from A_1 to the area A_2, thus increasing the positioning estimation accuracy of C_2.

In this paper, to decrease the size of the uncertain area in which the client is localized, we introduce new constraints elaborating on the neighboring locations.
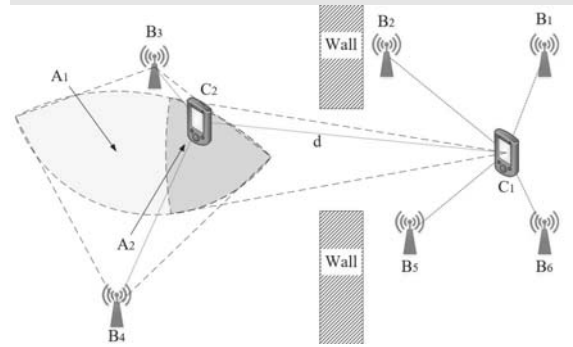

Fig. 2. Example of combined positioning for two clients.

The same scheme is also applied to one client case. We exploit the advantages of a combined positioning by introducing the concept of virtual positioning client (VPC) and using FTM ranging measurements retrieved from the client at previous locations. In Fig. 3 we show an example in which a client moves from position 1 to position 3 passing through position 2 ($P_1 \rightarrow P_2 \rightarrow P_3$). In correspondence of each position, the client performs FTM ranging actions. The proposed positioning system marks the three positions as VPC (V_1, V_2, V_3). Given the distances between VPCs, the position estimation accuracy of V_3 can be improved by elaborating the ranging measurements retrieved from V_3 and all the measurements collected from V_1 and V_2.

Knowing the previous VPC positions helps improve accuracy during the current VPC position estimation. Considering that the accurate distance between VPCs is unknown, our proposed system utilizes a moving distance estimation module to coarsely estimate the distances between VPCs. The number of distance-based constraints is equal to the number of adjacent VPC pairs. Assume m is the number of VPCs, then the number of estimated distances between VPCs is $m - 1$. For example, in Fig. 3, the distances between 3 VPCs, are the estimated distances between $V_2 \ and \ V_1$ ($\widehat{l_{2,1}}$) and $V_3 \ and \ V_2$ ($\widehat{l_{3,2}}$). These two distances are applied as spatial constraints in our method.
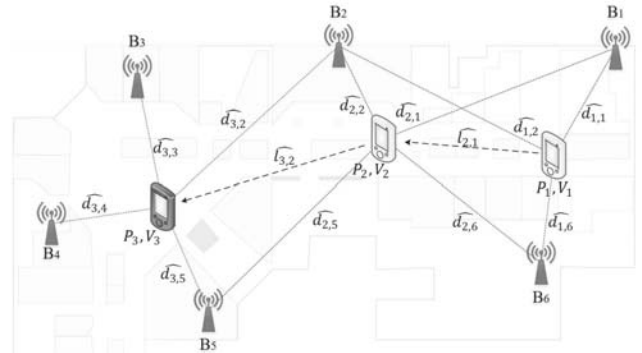

Fig. 3. Example of virtual positioning clients.

C. System Architecture

A positioning scenario in which the proposed positioning system can apply is as follows. A target client, for example, a user which carries an FTM certified smartphone, moves into an indoor environment. The client periodically sends FTM ranging requests to nearby FTM certified Wi-Fi APs which answer with an acknowledgment (ACK) frame so enabling the ranging evaluation. Then, the positioning client estimates itself position by evaluating the received ranging measurements.

The positioning method proposed in this paper relies on the spatial constraints of multiple positioning beacons displaced into the indoor environment. We convert a sequence of ranging measurements in the temporal domain into multiple VPCs in the spatial domain considering their spatial constraints. These VPCs are served as the positioning nodes. The current position estimation is the result of a combined optimization of multiple VPC positions. Indeed, by establishing a robust positioning objective function and the VPC spatial constraints expressed as KKT conditions, we evaluate the current position through a non-convex optimization. Finally, the system proposed includes an iterative ToF ranging and a VPC positioning weight estimation method to optimize the positioning model. The proposed system architecture, shown in Fig. 4, relies on six functional modules: the initial position estimation, the initial VPC creation, the weight estimation of ranging measurements, the weight estimation of VPCs, the KKT constrained optimization, and the client moving distance estimation.

Initial position estimation: this module measures the distance from the client to the nearby APs and then, by knowing the measurements and the position of the Wi-Fi APs, the module estimates the initial rough position of the target client. The module determines the position of the target client evaluating simultaneously range measurements from more than three Wi-Fi APs located at a known site. This procedure is known as trilateration [47]. We solve the initial position problem using the least square method.
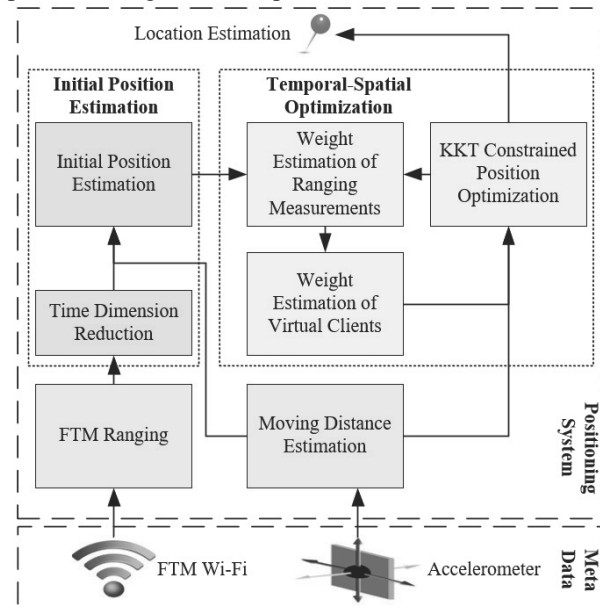

Fig. 4. Overview of the proposed system.

VPC creation: the function of this module is to transform a sequence of FTM gathered in the temporal domain into a series of VPCs and to evaluate their spatial constraints. These constraints are used to improve accuracy performances.

Weight estimation of ranging measurements: the module adjusts the weights of ranging measurements using robust statistics to reduce the influences of multipath effects.

Weight estimation of VPCs: when a mobile client moves, the interferences at different positions vary. Therefore, the weights of VPCs in the objective function should be tuned. The module estimates VPC weights using the information about the number of VPCs and ranging residuals.

KKT constrained optimization: this module evaluates errors from current and historical FTM ranging and estimates the possible moving distances of adjacent VPCs. It builds an objective function of VPC measurements, then it reduces the solution domain of the objective function considering the connections between VPCs.

Client moving distance estimation: the module estimates the distances between different VPCs. For example, an acceleration frequency-based step length model [48] can be applied to estimate the moving distance of a person who holds a smartphone terminal.

The overall process of the proposed positioning is shown in TABLE I. When a user moves, the positioning client collects FTM ranging measurements and construct VPCs. Then the system roughly estimates VPC initial positions. Based on the initial positions, we further improve the positioning accuracy with temporal-spatial optimizations.

TABLE I.   THE OVERALL POSITIONING ALGORITHM

1: **while TRUE**
2:     Get FTM ranging measurements
3:     Estimate the client's current position with FTM measurements
4:     Create VPCs
5:     Estimate the distances between the VPCs
6:     ***KKT Constrained Positioning Optimization***
7:     **repeat**
8:       Update the weight of FTM ranging measurements
9:       Update the weight of the estimated VPC positions
10:      Solve the temporal-spatial constrained optimization function with KKT conditions, and update the VPC position estimations.
11:    **until** the VPC position estimations converge.
12:    Output the latest VPC position as the current positioning result.
13: **end while**

IV. KKT Constrained Optimization with Temporal-spatial Models

This section models the multi-constraint positioning problem with KKT conditions and Lagrangian multipliers. Then we detail the key parameter estimation algorithms in the model, which is the Huber based robust ranging weight estimation and the VPC Weight Estimation.

A. KKT Constrained Temporal-Spatial Optimization

The initial positioning estimation can be improved by considering VPC temporal-spatial constraints. This section explains a KKT based method that is able to solve the constrained optimization problem. We analyze the key parameters that influence ranging quality and how to leverage

the quality coefficients in order to adjust the weights of the ranging during the positioning estimation process. The proposed algorithm is shown in TABLE 2.

Starting from the estimated initial position of VPCs, our algorithm updates the weights of ranging measurements $\omega_{i,j}$ and the weights of VPC position estimations ψ_i. Then, the system defines the objective function and temporal-spatial constraints. Successively, the optimization routine constructs the unconstrained Lagrangian and the KKT conditions. Finally, the system solves the objective function and update the VPC position estimations. For each loop, we calculate the average of VPC position variation distances δ. The variation average less than a fixed value means that the positioning result is converged and the system produces the final VPC position estimation as output.

TABLE 2. KKT CONSTRAINED POSITIONING OPTIMIZATION ALGORITHM

1: **Initialization**
2:    Input the estimated initial positions $\tilde{p}_i(i = 1, \dots, m)$ of VPCs
3:    Input the Wi-Fi beacon coordinates $\breve{p}_j(j = 1, \dots, n)$
4:    Input the available ranging measurements $\widehat{d_{i,j}}$
5: **Optimization Loop**
6: **repeat**
7:        Update ranging weight $\omega_{i,j}$ based on estimated VPC positions.
8:        Update VPC position weight ψ_i based on estimated VPC positions.
9:        Construct the objective function $J(\cdot)$
10:      Construct the temporal-spatial constraints
11:      Construct Lagrangian and KKT conditions
12:      Solve the objective function
13:      Update VPC position estimations
14   Calculate the average δ of VPC position variations of adjacent iterations.
15: **until** δ is small enough
16:   Output optimized VPC Positions.

We define the objective function of the optimization problem as the squared sum of the residual between the estimated distance and the FTM ranging measurement:

$$J(\widetilde{p_1}, \dots, \widetilde{p_m})$$
$$= \sum_{i=1}^{m} \psi_i(\cdot) \cdot \sum_{j=1}^{n} [\omega_{i,j}(\cdot) \cdot (\widehat{d_{i,j}} - \|\tilde{p}_i - \breve{p}_j\|_2)]^2 \quad (1)$$

where $\tilde{p}_i$ is the estimated position of the i_{th} VPC, $\breve{p}_j$ is the given position of the j_{th} Wi-Fi beacon, $\widehat{d_{i,j}}$ is the ranging measurement from $\tilde{p}_i$ to $\breve{p}_j$. Considering that the multipath effect varies at different positions, the ranging qualities of each measurement are different, therefore we add a weight estimation function $\omega_{i,j}(\cdot)$ to adjust the influence of the ranging qualities and a weight estimation function $\psi_i(\cdot)$ to adjust the influence of VPC position confidences. These two functions are discussed in the following sub-sections.

In order to improve the positioning performance, the system implements temporal-spatial constraints in order to decrease the definition domain of the objective function. These constraints restrict the possible position patterns of VPCs, therefore many error patterns are filtered out improving the system's performances.

VPC moving distance range constraints: when a user moves, the moving distance estimator module evaluates the distance between two consecutive VPCs. The estimator also provides a relative position relationship which restricts the possible position of the VPCs. Considering the difference in the accuracy of different moving distance estimation methods, we propose a ring definition domain to represent the above-mentioned restrictions as constraints. Therefore, we calculate the standard deviation σ_e of the moving distance estimation error and we use the error standard deviation as a constraint of the objective function. The moving distance of adjacent VPCs fall in the gap $(\widehat{l_{k,k+1}} - 2\sigma_e, \widehat{l_{k,k+1}} + 2\sigma_e,)$, where the parameter $\widehat{l_{k,k+1}}$ is the VPC moving distance estimation. The two constraints can be represented with the following equations:

$$g_{k,k+1}(\widetilde{p_k}, \widetilde{p_{k+1}}) = \|\tilde{p}_k - \widetilde{p_{k+1}}\|_2^2 - (\widehat{l_{k,k+1}} + 2\sigma_e)^2 \le 0 \quad (2)$$
$$\text{for } k = 1, \cdots, m-1$$

$$h_{k,k+1}(\widetilde{p_k}, \widetilde{p_{k+1}}) = (\widehat{l_{k,k+1}} - 2\sigma_e)^2 - \|\tilde{p}_k - \widetilde{p_{k+1}}\|_2^2 \le 0 \quad (3)$$
$$\text{for } k = 1, \cdots, m-1$$

Equation (2) and (3) restrict, respectively, the maximum and minimum bound of the moving distance between two consecutive VPCs. We utilize the two inequalities to constrain the possible scope of the VPC moving distance, rather than one equality to restrict the step length. The benefit is that the proposed method is adaptive to different moving distance estimation accuracies.

Positioning bound constraints: we consider the maximum and the minimum coordinates of all the Wi-Fi beacons to constrain the VPC positioning results.

$$\begin{cases} u_j^1(\tilde{x}_j) = \tilde{x}_j - x_{max} \le 0, \text{ for } j = 1, \cdots, m \\ u_j^2(\tilde{x}_j) = -\tilde{x}_j + x_{min} \le 0, \text{ for } j = 1, \cdots, m \\ u_j^3(\tilde{y}_j) = \tilde{y}_j - y_{max} \le 0, \text{ for } j = 1, \cdots, m \\ u_j^4(\tilde{y}_j) = -\tilde{y}_j + y_{min} \le 0, \text{ for } j = 1, \cdots, m \quad (4) \\ x_{max} = \max(x_1, \dots, x_n) \\ x_{min} = \min(x_1, \dots, x_n) \\ y_{max} = \max(y_1, \dots, y_n) \\ y_{min} = \min(y_1, \dots, y_n) \end{cases}$$

where the $x_{max}, x_{min}, y_{max}, y_{min}$ are the coordinate bound of Wi-Fi beacons. Then we utilize four equations $u_j^1, u_j^2, u_j^3, u_j^4$ to ensure the positioning results lies within the bound.

In order to solve the constrained optimization problem, we construct the Lagrange multiplier and the KKT conditions. Based on the objective function (1), and the constraint equations (2) ~ (4), the positioning problem can be represented as the following inequality constrained optimization:

$$\min_{\widetilde{p_1}, \dots, \widetilde{p_m}} J(\widetilde{p_1}, \dots, \widetilde{p_m})$$
$$s.t. \ g_{k,k+1}(\widetilde{p_k}, \widetilde{p_{k+1}}) \le 0, for \ k = 1, \cdots, m-1$$
$$h_{k,k+1}(\widetilde{p_k}, \widetilde{p_{k+1}}) \le 0, for \ k = 1, \cdots, m-1$$
$$u_j^1(\tilde{x}_j) \le 0, for \ j = 1, \cdots, m$$
$$u_j^2(\tilde{x}_j) \le 0, for \ j = 1, \cdots, m \quad (5)$$
$$u_j^3(\tilde{y}_j) \le 0, for \ j = 1, \cdots, m$$
$$u_j^4(\tilde{y}_j) \le 0, for \ j = 1, \cdots, m$$

The equation (5) represents that solving the positions of VPCs $\widetilde{p_1}, \ldots, \widetilde{p_m}$ is to find the minimum of the objective function $J(\cdot)$. We construct the unconstrained Language optimization function based on equation (5):

$$
\begin{aligned}
\mathcal{L}(&\widetilde{p_1}, \ldots, \widetilde{p_m}, \lambda_1, \ldots, \lambda_{m-1}, \eta_1, \ldots, \eta_{m-1}, \\
&\theta_1, \ldots, \theta_m, \xi_1, \ldots, \xi_m, \tau_1, \ldots, \tau_m, \gamma_1, \ldots, \gamma_m) \\
&= J + \sum_{k=1}^{m-1} (\lambda_k g_{k,k+1} + \eta_k h_{k,k+1}) \\
&\quad + \sum_{j=1}^{m} (\theta_j u_j^1 + \xi_j u_j^2 + \tau_j u_j^3 + \gamma_j u_j^4)
\end{aligned}
\tag{6}
$$

The parameter $\lambda_k, \eta_k \in \mathbb{R}$ for $k = 1, \cdots, m-1$ and $\theta_j, \xi_j, \tau_j, \gamma_j \in \mathbb{R}$ for $j = 1, \cdots, m$ are regularization items. The feasible positioning results can be resolved with the following KKT conditions:

$$
\begin{cases}
\nabla_{(\widetilde{x_1}, \widetilde{y_1}, \ldots, \widetilde{x_m}, \widetilde{y_m})} \mathcal{L}(\cdot) = 0 \\
\lambda_k g_{k,k+1} = 0, for\ k = 1, \cdots, m-1 \\
\eta_k h_{k,k+1} = 0, for\ k = 1, \cdots, m-1 \\
\theta_j u_j^1 = 0, for\ j = 1, \cdots, m \\
\xi_j u_j^2 = 0, for\ j = 1, \cdots, m \\
\tau_j u_j^3 = 0, for\ j = 1, \cdots, m \\
\omega_j u_j^4 = 0, for\ j = 1, \cdots, m \\
h_{k,k+1} \leq 0, g_{k,k+1} \leq 0, for\ k = 1, \cdots, m-1 \\
u_j^1 \leq 0, u_j^2 \leq 0, u_j^3 \leq 0, u_j^4 \leq 0, for\ j = 1, \cdots, m \\
\lambda_k \geq 0, \eta_k \geq 0, for\ k = 1, \cdots, m-1 \\
\theta_j \geq 0, \xi_j \geq 0, \tau_j \geq 0, \gamma_j \geq 0, for\ j = 1, \cdots, m \\
\nabla^{(2)}_{(\widetilde{x_1}, \widetilde{y_1}, \ldots, \widetilde{x_m}, \widetilde{y_m})} \mathcal{L}(\cdot)\ is\ positive\ definite
\end{cases}
\tag{7}
$$

It is worth noting that equation (7) only calculates feasible solutions. Therefore, when the Lagrangian $\mathcal{L}(\cdot)$ is not convex on the whole definition domain, equation (7) will output several local minimums that are satisfied with the KKT conditions. Our algorithm checks the corresponding value of the objective function (1), then selects the minimum value as the final result.

B. Ranging Weight Estimation

The serious multipath effect of the indoor environment and the narrow bandwidth of ranging radio frequency makes the FTM signal noisy and the measurements contain outliers (e.g. large ranging errors). Generally, the outliers are detected and removed. Unfortunately, the removing criteria are subjective and, potentially, good ranging measurements are deleted. Therefore, we propose that leveraging the mean/median estimation to adjust the weight parameter $\omega_{i,j}$ of the FTM ranging measurements.

The FTM ranging model can be represented as:

$$
\widehat{d_{i,j}} = \|p_i - \breve{p}_j\|_2 + \varepsilon
\tag{8}
$$

where $\breve{p}_j$ are the coordinates of the j_{th} Wi-Fi beacons. p_i are the ground truth coordinates of the i_{th} VPC. ε is the random measurement noise. $\|p_i - \breve{p}_j\|_2$ is the true Euclidean distance between the Wi-Fi beacon and the VPC. $\widehat{d_{i,j}}$ is the measured value of $\|p_i - \breve{p}_j\|_2$.

Wi-Fi FTM ranging is based on the signal flying time, therefore the ranging error distributions of different ranging distances can be approximated as independent and identically distributed (IID). Consequently, the positions of multiple VPCs are evaluated by maximizing the joint probability of different measurements of different VPC and Wi-Fi beacon pairs. Considering the ranging error ε of Equation (8), the maximum likelihood estimation of $p_1, \ldots, p_m$ is the solution of:

$$
\begin{cases}
\max\limits_{p_1, \ldots, p_m} \prod_{i=1}^{m} \prod_{j=1}^{n} f(r_{i,j}) = MAX \\
r_{i,j} = \widehat{d_{i,j}} - \|p_i - \breve{p}_j\|_2
\end{cases}
\tag{9}
$$

where $r_{i,j}$ represents the ranging residual. Adjusting the position of $p_1, \ldots, p_m$, when the joint probability reaches the maximum MAX, the positions are the optimal estimations $p_1, \ldots, p_m$ represented as $\widetilde{p_1}, \ldots \widetilde{p_m}$. When a ranging measurement is not available, the probability of this beacon and VPC pair is set to 1.

In order to simplify the evaluation cost of equation (9), the equation is transferred into a minimization problem:

$$
\begin{cases}
\widetilde{p_1}, \ldots \widetilde{p_m} = \min\limits_{p_1, \ldots, p_m} \sum_{i=1}^{m} \sum_{j=1}^{n} \rho(p_i) = MIN \\
\rho(p_i) = -\log\left(f(r_{i,j})\right) \\
MIN = -\log(MAX)
\end{cases}
\tag{10}
$$

Based on the robust statistics theory [12], we define the distribution f as a normal distribution if the residual r is smaller than a threshold T, or as a double exponential distribution otherwise.

$$
f(r_{i,j}) = \begin{cases}
\frac{1}{\sqrt{2\pi}} e^{-\frac{(r_{i,j})^2}{2}} & (|r_{i,j}| < T) \\
\frac{1}{2} e^{-|r_{i,j}|} & (|r_{i,j}| > T)
\end{cases}
\tag{11}
$$

Considering that the distributions of all the residuals are IID, the optimal solution of equation (10) is when all items of the equation reach their minimum value. Therefore, when f is subject to a normal distribution, the optimal $\widetilde{p_1}$ is at the point when its equation (11)'s derivative equals zero or, in other words. when the optimal point set of $\widetilde{p_1}$ lies in a circle with its radius equal to the mean of measurements $\widehat{d_{i,j}}$:

$$
\|p_i - \breve{p}_j\|_2 = mean(\widehat{d_{i,j}})
\tag{12}
$$

When f is subject to a double exponential distribution, the optimal $\widetilde{p_1}$ is the median value [12]:

$$
\|p_i - \breve{p}_j\|_2 = Med(\widehat{d_{i,j}})
\tag{13}
$$

and the optimal point set of $\widetilde{p_1}$ lies in a circle with its radius equal to the median of measurements $\widehat{d_{i,j}}$.

Because the sample median is more robust than the sample mean, we use the median value when the residual is greater than the threshold T. On the other hand, the median's robustness needs a higher sample price [12], therefore, we adopt mean estimation when the residual is small.

When the positioning client moves, the client only gets one sample per location. Consequently, it is difficult to adopt the mean/median estimations based on a single sample. Therefore,

we leverage the weight function to transfer the mean/median estimation into FTM ranging weights. Then, we can adopt robust statistics on multiple single measurements. The weight function is defined as [12]:

$$W(r_{i,j}) = \frac{d\rho}{dr_{i,j}}/r_{i,j} \qquad (14)$$

Adopting the definition to the equation (11). Therefore, the weight function $\omega_{i,j}(t)$ of FTM ranging is:

$$\omega_{i,j}(\cdot) = W(r_{i,j}) = \begin{cases} 1 & for\ |r_{i,j}| \leq T \\ T/|r_{i,j}| & for\ |r_{i,j}| > T \end{cases} \qquad (15)$$

Note that equation (15) depends on the p_i that represents the ground truth coordinates of the i_{th} VPC. Obviously, the ground truth coordinates are unknown in real-time positioning. In practice, we leverage the VPC position estimation of every iteration to replace the p_i, then we adjust the ranging weight during the next iteration of the algorithm.

C. VPC Weight Estimation

In order to further improve system positioning accuracies, the proposed system leverage the temporal-spatial constraints of multiple VPCs to shrink the feasible solution domain of the objective function (1). VPCs are located at different places, so the interference level of each VPC varies. Therefore, identifying the position confidence of each VPC and consequently adjust their weight is important in improving the evaluation of the objective function. Therefore, we propose a heuristic method to adjust the VPC weight ψ_i in equation (1).

Based on our experience, the number of ranging measurements and the accuracy of each ranging are the two key factors that decide the performance of VPC position estimation in trilateration. Obviously, more FTM ranging measurements are helpful in improving positioning robustness, because, with more measurements, outliers are more easily be identified. On the other hand, accurate ranging is the precondition of high accuracy positioning. The parameter $\omega_{i,j}(\cdot)$ is a robust weight estimation of the ranging residual, which just represents the confidence of each ranging measurement. Therefore, as equation (16) reveals, we propose that utilizing the sum of all the ranging weights of a VPC to represent the potential positioning confidence of the VPC.

$$\psi_i(\cdot) = \sum_{j=1}^{n} \omega_{i,j} \qquad (16)$$

V. IMPLEMENTATION AND EVALUATION

This section exhibits the performance of the proposed positioning system. It describes the experimental environment, platforms, and the key parameter of the algorithm. Finally, comprehensive performance tests are discussed and compared with state-of-the-art methods.

A. Experimental Environment

Because the IEEE 802.11mc protocol is newly proposed in Android 9, most of the off-the-shelf smartphones and Wi-Fi access points still not support the protocol yet. Therefore, we assemble experimental platforms by ourselves. As Fig. 5

reveals we use an Intel Dual Band Wireless-AC 8260 Wi-Fi card as the FTM ranging terminals because the card supports the IEEE 802.11mc protocol and open accessing FTM measurements. The card is mounted on a commercial desktop device in order to make it a beacon transmitter. We also replace the Wi-Fi card of a commercial DELL Inspiron 5488 with the same Intel 8260 card. In this case, the laptop serves as the target client. In order to expose the Wi-Fi antenna of the beacon transmitter, we extended the PCI-E slot of the beacon with an extension cable instead of extending the antenna. Because the signal traveling velocity in cables is different from the speed in vacuum [10], extending the cable does not introduce a time delay.
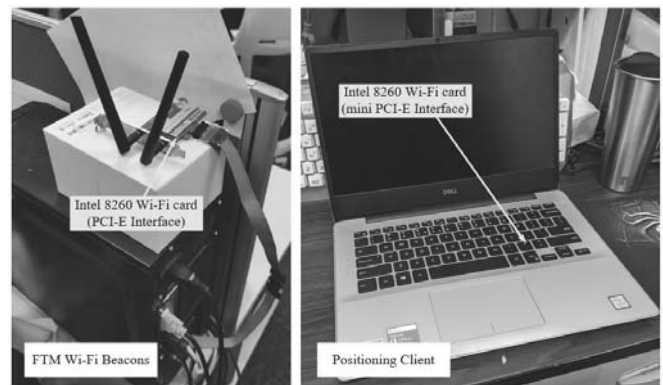

Fig. 5. Equipment of the proposed systems.

The operating system (OS) in both the Wi-Fi beacons transmitter and target client is Linux kernel version 3.19.0-61-low-latency because it is the only version that is supported by the backport LinuxCore releases of the IWLWIFI driver [10]. We configure the positioning nodes with the iw Linux command-line tool (the iw is an nl80211 based CLI configuration utility for wireless devices).

We chose to perform the experimental campaign in a real-world indoor environment where the multipath problem is complicated by reflections from walls, ceilings, doors, and furniture. The testbed is located on the seventh floor of an office building and it covers an area of $40m \times 15m$, with a ceiling of $3m$ high. The chosen area, as shown in Fig. 6, presents a challenging scenario, due to the dense number of workstations, chairs, a big iron plant rack standing in the middle of the positioning area, glass walls, and windows. These objects reflect FTM signals in various directions, thus causing serious multipath problems compared to an outdoor open space [10]. The electromagnetic environment is also complex due to the presence of many Wi-Fi access points, Bluetooth beacons, and personal computers. Our positioning system is configured ranging with 20MHz bandwidth in 2.4GHz. More than 200 normal Wi-Fi access points and Bluetooth beacons can be detected in this frequency, therefore the FTM ranging signal is interfered by these noises. A user held the client and walked along the testing path within the experiment area. The FTM sample frequency is 1Hz.
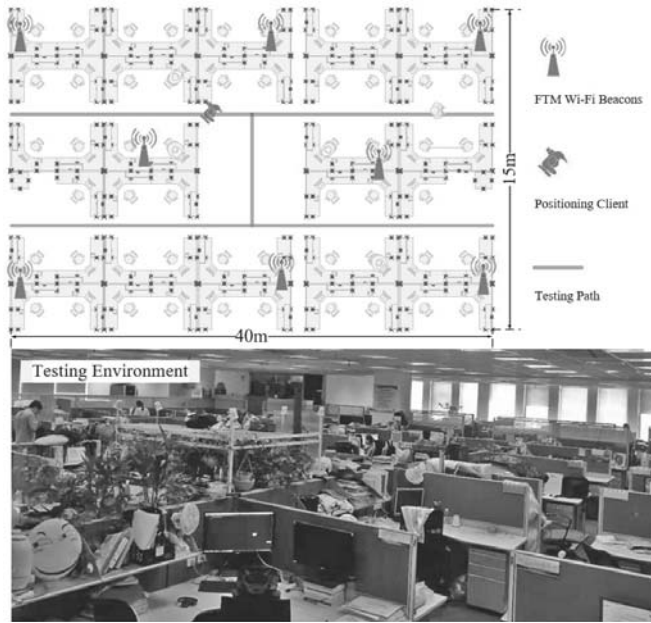
Fig. 6. A floor plan of our experimental office building. The bottom picture is a photo of the positioning area.

B. Impact of the VPC Moving Distance Estimation

The estimation accuracy of the user moving distance decides the range of the possible VPC moving distance formulated as KKT conditions. In this evaluation, we simulate different levels of estimation accuracies of the moving distance estimation module. We ask a user to randomly walk within the positioning area, the ground truth moving distance is extracted from the LiDAR measurements. Then, we simulate different grades of moving distance estimation accuracies comparing with the ground truth measurements. Given the ground truth moving distance L, the standard deviation σ_e of the moving distance estimation error is $L \cdot x\%$. We apply the constraints to the KKT condition equations (2) and (3). The goal of the experiment is to find out how the spatial constraints of adjacent VPCs affect the system positioning accuracy.
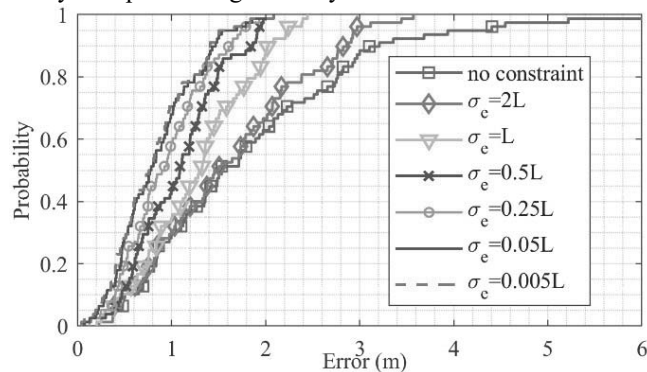

Fig. 7. The system positioning accuracy considering different VPC moving distance estimator accuracies

By repeating the same experiment for all the σ_e values, we found the optimal empirical σ_e value. The results are shown in Fig. 7. The minimum available σ_e is $2L$. When the estimator accuracy is too low, the spatial constraint expressed as KKT conditions have little effect on improving the positioning accuracy. When the estimator accuracy improves, the system positioning accuracy also increases, but the performances improve more slowly. When the estimator accuracy is higher than 0.05L, the improvement of the positioning accuracy is so low that it can be ignored, because other factors become the major sources of errors.

C. Impact of the Ranging and VPC Weight Parameter

In the second experiment, we evaluate the VPC weight estimation process and the effects of the mean/median estimation. Given threshold T the mean/median estimation, we calculate the positioning residual of each iteration. In order to generalize the selection of the threshold T, we choose the standard deviation σ of FTM ranging errors as an indicator of the threshold T. We set $T = \sigma \cdot x\%$. If the residual is greater than T, indicating that measurement is probably an outlier, we utilize the robust median estimation. Otherwise, we adopt the precise mean estimation. When the optimal threshold T is selected, we also compare the positioning performance with and without the VPC weight estimation.

First, we calculate the error standard deviation σ. In our experiment, considering all the FTM ranging errors, $\sigma = 2.5m$. Then, we repeat the same experiment for all the T values and found the optimal empirical T value. The results are shown in Fig. 8. When the threshold T is too small, for example, $T = 0.1\sigma$, the system performs a median estimation of all the FTM measurements, leading to low positioning accuracy, because the system cannot leverage the mean method to get a better ranging estimation. As the threshold become bigger, $T = 1.2\sigma$ for instance, the FTM ranging accuracy is improved as such as the positioning accuracy. However, when the T value is too big, the system apply the same value to all the FTM measurements, which equals tot adjusting the weight of the ranging measurements. Therefore, the CDF lines of the $T = 50\sigma$ and $T = constant$ are coincident.
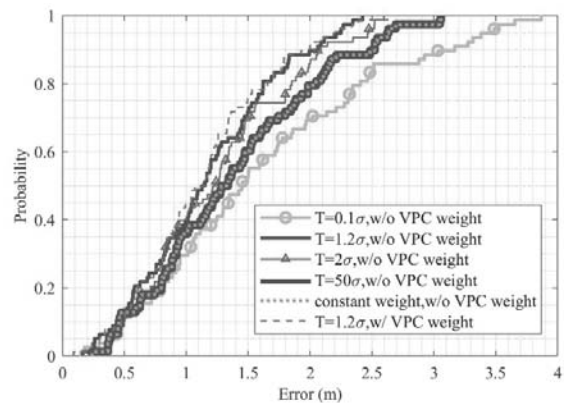

Fig. 8. The system positioning accuracy at different mean/median thresholds and the effects to apply the VPC weight estimation.

Furthermore, setting the threshold T equals to the optimal value 1.2σ, we apply the VPC weight estimation to the objective function (29). The result shows that although the improvement was small, the VPC weight estimation improves the overall positioning performance.

D. Number of VPC and Accumulative Error

In this section, we evaluate the impact on the positioning performances when different numbers of VPCs are considered. Fig. 9(a) shows the positioning performances by repeating the same evaluation and varying the number of VPCs from 2 to 9. The positioning accuracy increases as more VPCs are involved. The result confirms that increasing the number of VPCs is helpful in reducing the influence of the multipath effect. The multipath effect is location-related and VPCs are evaluated at different locations. When more VPCs are involved, the risk that all VPCs during a positioning request suffer from serious multipath effects is decreased. Therefore, although the proposed method decreases the weight of poor measurements, there are still enough ranging measurements to improve positioning accuracy.

It is worth noting that the accuracy improvement from 4 to 6 VPCs is slower than the improvement from 2 to 4 VPCs. When the number of VPCs exceeds 6, more VPCs produce little accuracy improvements. The phenomena confirm that as the number of VPCs increases, the influence of accumulative error from VPC distance estimations become prominent. The proposed algorithm leverages the constraints of multiple estimated distances between VPCs to shrink the solution space. Nevertheless, the accumulative error increases when more VPCs are involved. When the benefits from introducing VPC distance constraints and the harm from the accumulative errors of VPC distance estimations are balanced, the system positioning improvement stops. Therefore, in order to control the influence of the accumulative error, we implement a sliding window to only select the latest VPCs considered into the objective function evaluation.

Furthermore, increasing the number of VPCs enlarges the computing cost. As Fig. 9 (b) reveals the mean computation time is linear for different VPCs because the KKT condition is linear. On the other hand, the average time gap between the first and third quartile also enlarges as the VPC number increases, indicating that while the number of VPC spatial constraints increases, the variation of the problem complexity also enlarges.
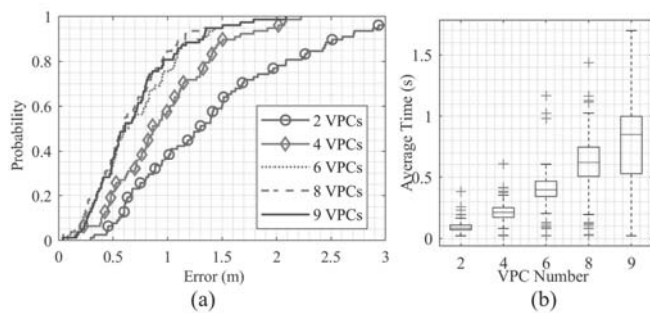

Fig. 9. (a) The positioning accuracy considering a different amount of VPC, (b) the running time statistics.

E. Performance with a different number of APs

Increasing the density of APs is an effective way to improve system positioning accuracy. As previously described, the experimental environment contains 8 APs deployed according to Fig.6(a). We collect ranging measurements from all the APs.

Then, in this experiment, we randomly reduce the number of APs and their corresponding ranging measurements.

We test the positioning performance using from 4 to 8 APs, respectively. As Fig. 10 shows, the positioning accuracy improves as the number of APs increases. Considering more APs lead to evaluate more spatial constraints in the solution space and to reduce the influence of ranging errors so improving the positioning accuracy. However, the proposed algorithm obtains accurate positioning performances also with a lower number of APs making the system applicable in different indoor environments.
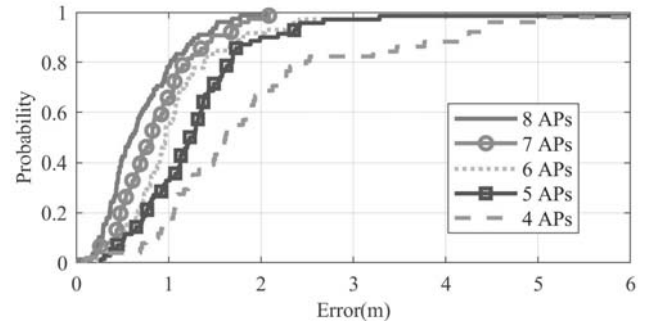

Fig. 10. The positioning accuracy according to different numbers of APs.

F. Convergence rate

The proposed algorithm is composed of an iterative routine that optimizes temporal-spatial measurements, which may have downsides when the convergence rate is low. In this section, we evaluate several key parameters that may affect system performance.

We examine the positioning accuracy obtained with a different number of iterations. Fig. 11 shows the log_{10} of error (error in meters) per iteration, given 8 VPCs. When the system is initialized applying the least square method, the median error is more than 5 meters, and due to ranging outliers, we observe errors up to more than 100 meters. Then, after the initialization, the median and maximum errors drop to 0.64 m and 2.1m respectively, indicating that the measurement weights have been properly adjusted and the outlier measurements have been effectively removed. However, when more iterations are performed the accuracy improvement becomes very small. The results show that the main improvement of positioning accuracy occurs at the first iteration.
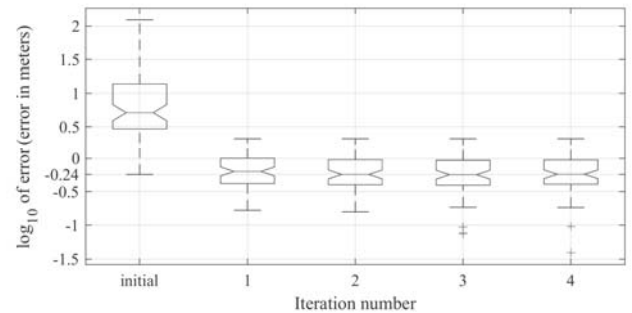

Fig. 11. The positioning error under a different number of iterations.

Then, we perform an ablation study [49] by applying different experimental conditions and we find two key factors

that affect the algorithm convergence rate: the number of VPCs, and the iteration stop threshold δ applied during the analysis of the variation of the VPC position. We observe the number of iterations adopting a different number of VPCs, given an iteration stop threshold $\delta = 0.67$. As Fig. 12 reveals the required number of iterations is proportional to the number of VPCs because more VPCs contain more ranging measurements. Basically, the problem becomes more complex when more ranging measurements are included, therefore, the number of required iterations is increased. Finally, we observe the number of iterations using different stop threshold δ, given 8 VPCs. Fig. 13 reveals that the required number of iterations is inversely proportional to the iteration stop threshold δ, because the system needs more iterations to reduce the variations of the VPC position. However, the accuracy improvement is very small after the first two iterations as shown in Fig.11, thus the choice of the iteration stop threshold can vary. Based on our experience, choosing a δ that keeps the median of iteration number equals two is a proper value (e.g. the $\delta = 0.67$ in Fig. 13).
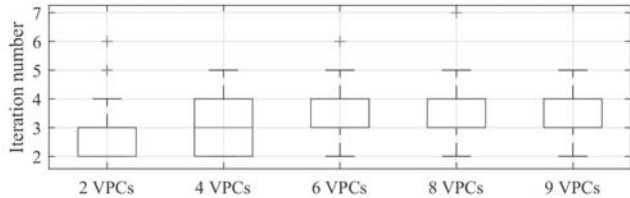

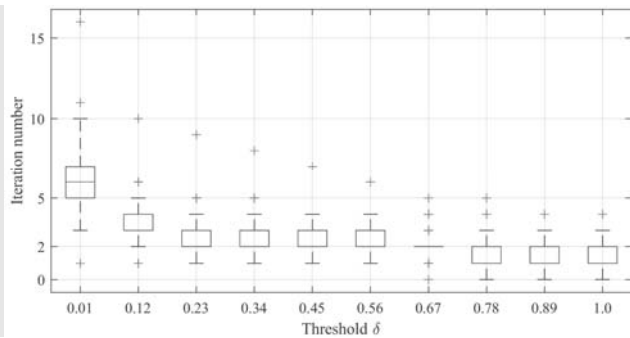Fig. 12.   Iteration number of different VPCs.

Fig. 13.   Iteration number with different position variation thresholds.

We conclude that our proposed algorithm can converge within two iterations for most of the cases. In order to examine whether the algorithm is able to converge within a reasonably short time, we calculate the average running time of one iteration under different circumstances. From our experiments, we find that the average iteration time is relevant to the number of available ranging measurements and the index of the iteration. Considering that the successful ranging rate of different VPCs varies, the number of available ranging measurements (e.g., in Fig. 3, V_1, V_2, V_3 retrieved 3, 3, and 4 measurements respectively, the total number of available ranging measurements is 10) is a precise metric for evaluating the complexity of the position optimization. In this experiment, we classify the number of measurements into five groups: 6~15, 16~25, 26~35, 36~45, 46~55, then we calculate the average running time of each iteration. The result is shown in Fig. 14.

It can be observed that considering an iteration index, the average running time shows a linear trend related to the number of ranging measurements. On the other hand, considering a number of available ranging measurements, the running time decreases as the iteration index increases. In fact, the algorithm uses a KKT routine to solve the KKT equations through sequential quadratic programming [50], and the running time is relevant during the evaluation of the initial position. Therefore, when the solution is close to the optimal, the running time decreases.
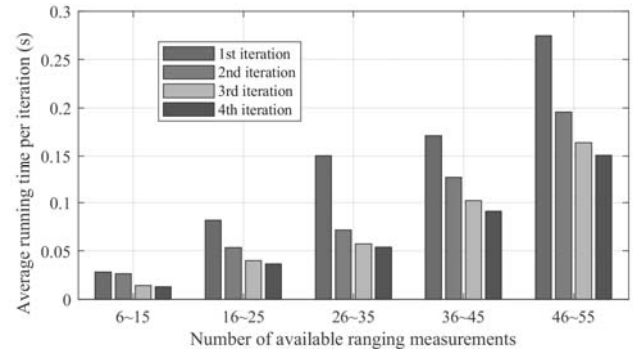

Fig. 14.   Average running time with different available ranging measurements.

In conclusion, in order to make the algorithm converge in a reasonably short time, it is important to select a proper number of VPCs and select the top-n ranging measurements based on their qualities, especially for scenarios with a large amount of FTM enabled APs.

G. Performance comparison with other FTM RTT-based positioning Methods

We evaluated the positioning performance comparing different Wi-Fi FTM RTT-based positioning approaches, namely, the least square (LS), robust LS, position regression neural network (PRNN), ranging error compensation neural network (RECNN), multi-dimension scaling (MDS) with the proposed positioning method (using 6 VPCs). The LS and MDS are classical positioning methods that implement triangulation with equal weight ranging measurements. The robust LS updates the classical LS to reduce the effect of multipath problems. This method is an iterative algorithm that adjusts the weight of ranging measurements in each iteration. We also tried the state-of-the-art artificial intelligence methods. The PRNN is a stack-structured artificial neural network (ANN) that maps a set of FTM measurements into VPC positions. The neural network consists of three layers and the adjacent layers are fully connected. We also add sa rectified linear unit (ReLu) neuron at each layer to deal with the nonlinearity. We sampled ground truth positions and trained the PRNN with a back-propagation algorithm. In the positioning phase, the PRNN receives the FTM measurements as inputs and predicts position regression results. The RECNN is similar to the PRNN, the difference is that the RECNN outputs are ranging error compensations and it compensates FTM ranging measurements and positioning through the LS method. We also compared the performance of traditional RSS based methods [5].

The results of the comparison are shown in Fig. 15. The traditional RSS based positioning method is worse than any other FTM based methods because the positioning oriented FTM protocol provides more location-related information. The performance of the LS method is the worst FTM positioning method because the LS method is easily affected by ranging outliers. The serious multipath effect in indoor environments generates lots of ranging errors, therefore the performance of the indoor least square method drops comparing to outdoor environments. The performance of the MDS method is better than the LS method because the coordinate alignment eliminates the effect of ranging outliers to a certain degree. The PRNN and RECNN method improve positioning performance because the training process enables the system to find outliers. However, the multipath effect at different positions changes significantly. Therefore, a large number of training samples to prevent overfitting problems is needed, which increases the deployment cost. The difference between the proposed method and the robust LS method is that the robust least square method does not consider the temporal-spatial constraints of VPCs. The robust LS method performs better than other methods because it also considers the weight of FTM ranging. Our proposal also leverages the temporal-spatial constraints of adjacent VPCs, which improves the system's capability to reduce the influence of FTM ranging outliers. Therefore, the proposed method reaches a sub-meter level of positioning accuracy at 80% in complex indoor environments.
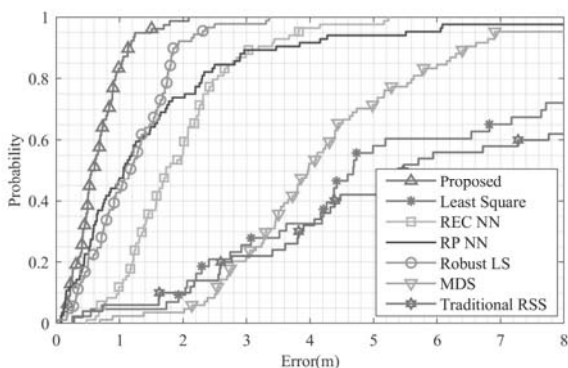

Fig. 15. Positioning performance comparison with different Wi-Fi FTM positioning methods.

VI. CONCLUSION

In this paper, we propose a robust indoor positioning method based on Wi-Fi FTM RTT measurements. Our algorithm relies on the temporal-spatial constraints between adjacent VPCs. The technique provides robust localization accuracy in a complex indoor environment in which the multipath effect and signal interferences are serious.

The main contributions of our work are three-fold. We convert the real-time position estimation problem into multiple VPC combined position optimization to reduces the multipath effect. We establish the VPC spatial constrained Karush–Kuhn–Tucker conditions to model the constrained objective functions. Finally, we propose an iterative ToF ranging and VPC weight estimation method to optimize the positioning model. Initial experiments using open platform wireless cards

have confirmed that our novel scheme improves the positioning performances significantly if compared to classical positioning methods.

REFERENCES

[1] M. Yang, L. Chuo, K. Suri, L. Liu, H. Zheng, and H. Kim, "iLPS: Local Positioning System with Simultaneous Localization and Wireless Communication," in *IEEE INFOCOM 2019 - IEEE Conference on Computer Communications*, 29 April-2 May 2019 2019, pp. 379-387, doi: 10.1109/INFOCOM.2019.8737569.

[2] H. Zou, Y. Zhou, J. Yang, and C. J. Spanos, "Unsupervised WiFi-Enabled IoT Device-User Association for Personalized Location-Based Service," *IEEE Internet of Things Journal,* vol. 6, no. 1, pp. 1238-1245, 2019, doi: 10.1109/JIOT.2018.2868648.

[3] J. Hu, D. Liu, Z. Yan, and H. Liu, "Experimental Analysis on Weight K-Nearest Neighbor Indoor Fingerprint Positioning," *IEEE Internet of Things Journal,* vol. 6, no. 1, pp. 891-897, 2019, doi: 10.1109/JIOT.2018.2864607.

[4] N. Yu, X. Zhan, S. Zhao, Y. Wu, and R. Feng, "A Precise Dead Reckoning Algorithm Based on Bluetooth and Multiple Sensors," *IEEE Internet of Things Journal,* vol. 5, no. 1, pp. 336-351, 2018, doi: 10.1109/JIOT.2017.2784386.

[5] S. Yang, P. Dessai, M. Verma, and M. Gerla, "FreeLoc: Calibration-free crowdsourced indoor localization," in *2013 Proceedings IEEE INFOCOM*, Turin, Italy, 14-19 April 2013 2013, WiFi pp. 2481-2489, doi: 10.1109/INFCOM.2013.6567054.

[6] P. Bahl and V. N. Padmanabhan, "RADAR: An in-building RF-based user location and tracking system," in *INFOCOM 2000. Nineteenth Annual Joint Conference of the IEEE Computer and Communications Societies. Proceedings. IEEE*, Tel Aviv, Israel, Israel, 2000, vol. 2, WiFi Ieee, pp. 775-784.

[7] C. Wu, Z. Yang, Y. Liu, and W. Xi, "WILL: Wireless indoor localization without site survey," *IEEE Transactions on Parallel and Distributed Systems,* vol. 24, no. 4, pp. 839-848, 2012.

[8] I. W. Group, "IEEE standard for information technology–Telecommunications and information exchange between systems–Local and metropolitan area networks–Specific requirements–Part 11: Wireless LAN Medium Access Control (MAC) and Physical Layer (PHY) specifications Amendment 6: Wireless Access in Vehicular Environments," *IEEE Std,* vol. 802, no. 11, 2010.

[9] L. Banin, U. Schatzberg, and Y. Amizur, "Next Generation Indoor Positioning System Based on WiFi Time of Flight," in *Proc. 26th Int. Tech. Meeting Satellite Division Inst. Navigat.(ION GNSS+)*, 2013, vol. 2, pp. 975-982.

[10] M. Ibrahim *et al.*, "Verification: Accuracy Evaluation of WiFi Fine Time Measurements on an Open Platform," presented at the Proceedings of the 24th Annual International Conference on Mobile Computing and Networking, New Delhi, India, 2018.

[11] E. De Klerk, C. Roos, and T. Terlaky, "Nonlinear Optimization," ed: Citeseer, 2004.

[12] R. A. Maronna, R. D. Martin, V. J. Yohai, and M. Salibián-Barrera, *Robust statistics: theory and methods (with R)*. John Wiley & Sons, 2019.

[13] W. Shao *et al.*, "Location Fingerprint Extraction for Magnetic Field Magnitude Based Indoor Positioning," *J. Sens.,* vol. 2016, p. 16, 2016, Art no. 1945695, doi: 10.1155/2016/1945695.

[14] W. Shao, H. Luo, F. Zhao, C. Wang, A. Crivello, and M. Z. Tunio, "Mass-centered weight update scheme for particle filter based indoor pedestrian positioning," in *2018 IEEE Wireless Communications and Networking Conference (WCNC)*, Barcelona, Spain, 15-18 April 2018 2018, pp. 1-6, doi: 10.1109/WCNC.2018.8377274.

[15] L. Gong, Y. Zhao, C. Xiang, Z. Li, C. Qian, and P. Yang, "Robust light-weight magnetic-based door event detection with smartphones," *IEEE Transactions on Mobile Computing,* vol. 18, no. 11, pp. 2631-2646, 2018.

[16] K. Liu, X. Liu, and X. Li, "Guoguo: Enabling Fine-grained Indoor Localization via Smartphone," *MobiSys*, p. 14, June 25-28, 2013. [Online]. Available: http://128.227.119.200/lkk/?page_id=7.

[17] W. Shao, H. Luo, F. Zhao, C. Wang, A. Crivello, and M. Z. Tunio, "DePedo: Anti Periodic Negative-Step Movement Pedometer with Deep Convolutional Neural Networks," in *2018 IEEE International*

Conference on Communications (ICC), Kansas City, MO, USA, 20-24 May 2018 2018, pp. 1-6, doi: 10.1109/ICC.2018.8422308.

[18] W. Shao, H. Luo, F. Zhao, and A. Crivello, "Toward improving indoor magnetic field–based positioning system using pedestrian motion models," *Int J Distrib Sens N,* vol. 14, no. 9, p. 1550147718803072, 2018, doi: 10.1177/1550147718803072.

[19] K. Kale, S. Pawar, and P. Dhulekar, "Moving object tracking using optical flow and motion vector estimation," in *2015 4th International Conference on Reliability, Infocom Technologies and Optimization (ICRITO) (Trends and Future Directions)*, 2-4 Sept. 2015 2015, Camera, pp. 1-6, doi: 10.1109/ICRITO.2015.7359323.

[20] R. Faragher and R. Harle, "An analysis of the accuracy of bluetooth low energy for indoor positioning applications," in *Proceedings of the 27th International Technical Meeting of the Satellite Division of the Institute of Navigation (ION GNSS+'14)*, 2014, BLE, pp. 201-210.

[21] W. Shao, H. Luo, F. Zhao, Y. Ma, Z. Zhao, and A. Crivello, "Indoor positioning based on fingerprint-image and deep learning," *IEEE Access,* pp. 1-1, 2018, doi: 10.1109/ACCESS.2018.2884193.

[22] A. Khalajmehrabadi, N. Gatsis, and D. Akopian, "Modern WLAN Fingerprinting Indoor Positioning Methods and Deployment Challenges," *IEEE Communications Surveys & Tutorials,* vol. 19, no. 3, pp. 1974-2002, 2017, doi: 10.1109/COMST.2017.2671454.

[23] C. Wu, Z. Yang, and C. Xiao, "Automatic radio map adaptation for indoor localization using smartphones," *IEEE Transactions on Mobile Computing,* vol. 17, no. 3, pp. 517-528, 2017.

[24] S. He and S.-H. G. Chan, "Tilejunction: Mitigating signal noise for fingerprint-based indoor localization," *IEEE Transactions on Mobile Computing,* vol. 15, no. 6, pp. 1554-1568, 2015.

[25] S.-H. Fang and T. Lin, "Principal component localization in indoor WLAN environments," *IEEE Transactions on Mobile Computing,* vol. 11, no. 1, pp. 100-110, 2011.

[26] P. Mirowski, H. Steck, P. Whiting, R. Palaniappan, M. MacDonald, and T. K. Ho, "KL-divergence kernel regression for non-Gaussian fingerprint based localization," in *2011 International Conference on Indoor Positioning and Indoor Navigation*, 2011: IEEE, pp. 1-10.

[27] C. Feng, W. S. A. Au, S. Valaee, and Z. Tan, "Received-signal-strength-based indoor positioning using compressive sensing," *IEEE Transactions on mobile computing,* vol. 11, no. 12, pp. 1983-1993, 2011.

[28] A. Khalajmehrabadi, N. Gatsis, D. J. Pack, and D. Akopian, "A joint indoor WLAN localization and outlier detection scheme using LASSO and elastic-net optimization techniques," *IEEE Transactions on Mobile Computing,* vol. 16, no. 8, pp. 2079-2092, 2016.

[29] J. Xiong and K. Jamieson, "Arraytrack: A fine-grained indoor location system," in *Presented as part of the 10th {USENIX} Symposium on Networked Systems Design and Implementation ({NSDI} 13)*, 2013, pp. 71-84.

[30] S. Kumar, S. Gil, D. Katabi, and D. Rus, "Accurate indoor localization with zero start-up cost," in *Proceedings of the 20th annual international conference on Mobile computing and networking*, 2014, pp. 483-494.

[31] M. Kotaru, K. Joshi, D. Bharadia, and S. Katti, "Spotfi: Decimeter level localization using wifi," in *Proceedings of the 2015 ACM Conference on Special Interest Group on Data Communication*, 2015, pp. 269-282.

[32] J. Gjengset, J. Xiong, G. McPhillips, and K. Jamieson, "Phaser: Enabling phased array signal processing on commodity WiFi access points," in *Proceedings of the 20th annual international conference on Mobile computing and networking*, 2014, pp. 153-164.

[33] Y. Xie, Z. Li, and M. Li, "Precise power delay profiling with commodity Wi-Fi," *IEEE Transactions on Mobile Computing,* vol. 18, no. 6, pp. 1342-1355, 2018.

[34] J. Xiong, K. Sundaresan, and K. Jamieson, "Tonetrack: Leveraging frequency-agile radios for time-based indoor wireless localization," in *Proceedings of the 21st Annual International Conference on Mobile Computing and Networking*, 2015, pp. 537-549.

[35] D. Vasisht, S. Kumar, and D. Katabi, "Decimeter-level localization with a single WiFi access point," in *13th {USENIX} Symposium on Networked Systems Design and Implementation ({NSDI} 16)*, 2016, pp. 165-178.

[36] W. Gong and J. Liu, "SiFi: Pushing the limit of time-based WiFi localization using a single commodity access point," *Proceedings of*

the ACM on Interactive, Mobile, Wearable and Ubiquitous Technologies, vol. 2, no. 1, pp. 1-21, 2018.

[37] A. Günther and C. Hoene, "Measuring round trip times to determine the distance between WLAN nodes," in *International conference on research in networking*, 2005: Springer, pp. 768-779.

[38] M. Ciurana, F. Barcelo-Arroyo, and F. Izquierdo, "A ranging system with IEEE 802.11 data frames," in *2007 IEEE Radio and Wireless Symposium*, 2007: IEEE, pp. 133-136.

[39] D. Giustiniano and S. Mangold, "CAESAR: carrier sense-based ranging in off-the-shelf 802.11 wireless LAN," in *Proceedings of the Seventh COnference on emerging Networking EXperiments and Technologies*, 2011: ACM, p. 10.

[40] U. Schatzberg, L. Banin, and Y. Amizur, "Enhanced WiFi ToF indoor positioning system with MEMS-based INS and pedometric information," in *2014 IEEE/ION Position, Location and Navigation Symposium - PLANS 2014*, 5-8 May 2014 2014, pp. 185-192, doi: 10.1109/PLANS.2014.6851374.

[41] L. Banin, O. Bar-Shalom, N. Dvorecki, and Y. Amizur, "Scalable Wi-Fi Client Self-Positioning Using Cooperative FTM-Sensors," *Ieee T Instrum Meas,* pp. 1-13, 2018, doi: 10.1109/TIM.2018.2880887.

[42] N. Dvorecki, O. Bar-Shalom, L. Banin, and Y. Amizur, "A Machine Learning Approach for Wi-Fi RTT Ranging," in *Proceedings of the 2019 International Technical Meeting of The Institute of Navigation*, Hyatt Regency Reston, Reston Virginia., 2019, doi: 10.33012/2019.16702.

[43] D. Giustiniano, T. Bourchas, M. Bednarek, and V. Lenders, "Deep Inspection of the Noise in WiFi Time-of-Flight Echo Techniques," presented at the Proceedings of the 18th ACM International Conference on Modeling, Analysis and Simulation of Wireless and Mobile Systems, Cancun, Mexico, 2015.

[44] M. Rea, A. Fakhreddine, D. Giustiniano, and V. Lenders, "Filtering Noisy 802.11 Time-of-Flight Ranging Measurements From Commoditized WiFi Radios," *IEEE/ACM Transactions on Networking,* vol. 25, no. 4, pp. 2514-2527, 2017, doi: 10.1109/TNET.2017.2700430.

[45] Y. Yu, R. Chen, L. Chen, G. Guo, F. Ye, and Z. Liu, "A Robust Dead Reckoning Algorithm Based on Wi-Fi FTM and Multiple Sensors," *Remote Sensing,* vol. 11, no. 5, p. 504, 2019. [Online]. Available: http://www.mdpi.com/2072-4292/11/5/504.

[46] U. Niesen, V. N. Ekambaram, J. Jose, and X. Wu, "Intervehicle Range Estimation From Periodic Broadcasts," *Ieee T Veh Technol,* vol. 66, no. 12, pp. 10637-10646, 2017, doi: 10.1109/TVT.2017.2762242.

[47] F. Thomas and L. Ros, "Revisiting trilateration for robot localization," *Ieee T Robot,* vol. 21, no. 1, pp. 93-101, 2005.

[48] P. Davidson and R. Piché, "A Survey of Selected Indoor Positioning Methods for Smartphones," *IEEE Communications Surveys & Tutorials,* vol. 19, no. 2, pp. 1347-1370, 2017, doi: 10.1109/COMST.2016.2637663.

[49] R. Meyes, M. Lu, C. W. de Puiseau, and T. Meisen, "Ablation studies in artificial neural networks," *arXiv preprint arXiv:1901.08644,* 2019.

[50] R. H. Byrd, J. C. Gilbert, and J. Nocedal, "A trust region method based on interior point techniques for nonlinear programming," *Mathematical programming,* vol. 89, no. 1, pp. 149-185, 2000.

Wenhua Shao is currently a postdoctoral researcher at the School of Software Engineering, Beijing University of Posts and Telecommunications (SSE-BUPT), Beijing, China. He is also a research assistant at the Institute of Computing Technology, Chinese Academy of Science (ICT-CAS), Beijing, China. His current main interests include location-based services, indoor localization, inertial navigation, pervasive computing, neural networks, and machine learning.

Haiyong Luo is an Associate Professor at the Institute of Computing Technology, Chinese Academy of Science (ICT-CAS), Beijing, China. His main research interests are location-based services, pervasive computing, mobile computing and the internet of things.

Fang Zhao is a Professor at the School of Software Engineering, Beijing University of Posts and Telecommunications (SSE-BUPT), Beijing, China. Her research Directions are Key technology of things, short-range wireless positioning, innovative mobile Internet applications, and mobile information.

Hui Tian (M'03) received the M.S. degree in microelectronics and the Ph.D. degree in circuits and systems from the Beijing University of Posts and Telecommunications in 1992 and 2003, respectively. She is a Professor with BUPT and the Director of the State Key Laboratory of Networking and Switching Technology. She is a Committee Member of the Beijing Key Laboratory of Wireless Communication Testing Technology, a Core Member of the Innovation group of the National Natural Science Foundation of China, a member of the China Institute of Communications, and an expert in the Unified Tolling and Electronic Toll Collection Working Group of the China National Technical Committee on ITS Standardization. Her research interests include LTE and 5G system design, MAC protocols, resource scheduling, cross-layer design, cooperative relaying in cellular systems, and ad hoc and sensor networks. She was a co-recipient of the National Award for Technological Invention, the Science and Technology Award of China Communications, and 10 major scientific and technological progresses Awards of China's colleges and Universities for her contribution in the field of wireless communication. She was a Lead Guest Editor for the EURASIP Journal on Wireless Communications and Networking. She has been a TPC Member for IEEE conferences (GlobalCom, WCNC, WPMC, PIMRC, VTC, ICCC, etc.) and the reviewer for IEEE TVT, IEEE CL, IET Communications, Transactions on Emerging Telecommunications Technologies, the EURASIP Journal on Wireless Communications and Networking, the Journal of Networks, the Majlesi Journal of Electrical Engineering, the Journal of China University of Posts and Telecommunications, the Chinese Journal of Electronics, the Journal of Electronics and Information Technology, the Chinese Journal of Aeronautics, etc.

Shuo Yan received a B.S. degree in software engineering from Beijing University of Posts and Telecommunications, Beijing, China, in 2017. He is currently pursuing an M.S. degree in software engineering from Beijing University of Posts and Telecommunications, Beijing. From 2017 to 2019, he was a Research Assistant in the Institute of Computing Technology, Chinese Academy of Sciences, Beijing, China. His main research interests are wireless indoor positioning and navigation using built-in sensors in smartphones, which includes WLAN, magnetic fields, fine time measurement, and artificial neural networks.

Antonino Crivello is a researcher at the Information Science and Technology Institute, Consiglio Nazionale delle Ricerche (ISTI-CNR), Pisa, Italy. He received his PhD degree in Information Engineering and Science from the University of Siena, Italy, in 2018. His research interests include Active and Assisted Living and Indoor Localisation.